

# Tri-band Impedance Matching Network Design Using Particle Swarm Optimization Algorithm

Sadık ÜLKER

*Electrical and Electronics Engineering Department, European University of Lefke, Gemikonağı,  
Lefke, Mersin – 10, Turkey  
sulker@eul.edu.tr*

**Abstract**—A solution strategy is presented using a five-section transmission line impedance transformer aiming for multiple band matching network circuits. In this paper, the analysis, which is based on the transmission line theory and application of the evolutionary algorithm for the solution of the stated problem are explained. Design of the matching networks was performed and optimized at three different frequencies 1.8 GHz, 2.4 GHz and 3 GHz at the same time. Tests were performed for two different load configurations. The optimized design values obtained from the particle swarm optimization algorithm were verified for correctness using microwave simulator. After the fabrication of the circuits, the measurements were taken for these circuits for the validation of the design. From the observations that were made, it can be concluded that particle swarm optimization can be a good choice for the design and optimization of multiple band matching network circuits.

**Index Terms**—computer aided engineering, evolutionary computation, impedance matching, microwave circuits, particle swarm optimization.

## I. INTRODUCTION

Impedance matching circuits play a crucial part in microwave engineering for enabling circuits to achieve maximum power transfer. Impedance matching techniques can be characterized into two main categories in terms of types of matching networks; lumped matching networks and transmission line matching networks. Lumped matching networks are usually preferred for low frequency applications due to the availability of lumped components and also usually are suitable for matching at single frequencies. Transmission line matching networks, however, are usually preferred because of their availability in lower and higher frequencies as well as their adaptability to multiple band circuits.

A single section, quarter wavelength long, transmission line can be used to match real load impedance at a single frequency. If the load is complex, we can use two section transmission lines with different characteristic impedances and lengths to achieve this kind of matching. Another alternative can be the application of shunt stub matching technique.

If the matching is required at a couple of different frequencies at the same time, the addition of multiple section transmission lines can be a method. Different techniques were presented in the past for solving the matching problem at different frequencies. A three section transmission line transformer extended from a two section concept was investigated by Chongcheawchamnan et al. [1].

A match for real load at three independent frequencies using stubbed coupling line was suggested by Wang et al. [2]. Another three band matching technique using modified T-type impedance transformers was proposed by Hu et al. [3]. For a dual band operation matching network design with multi-section transmission lines using particle swarm optimization was suggested and validated by Khodier et al. [4]. Design of triple-band impedance transformers using Z-transform techniques was proposed by Tsai [5-6] and the synthesis of unequal length multi-section transmission lines for multiband applications was investigated by Kim and Lee [7].

Besides doing research on different methodologies in matching circuits, different optimization techniques were used in microwave circuits. Li et al. used reactive matching circuit networks to optimize circuits without the need for switches on mobile phones [8]. Sami et al. proposed tri-band microstrip antenna design for wireless applications using a microwave simulator and genetic algorithm [9]. Chongcheawchamnan et al. used multi-section transmission lines in designing tri-band Wilkinson power divider [10]. They analyzed the circuit and derived a model for tri-band operation. For multi-band optimization, Dib and Khodier used particle swarm optimization technique for dual band, triple band and quad band power dividers [11].

In the design of dual band gridded-square and a triple band gridded-double-square array, frequency selective surfaces differential evolution strategy was proposed by Luo [12]. Particle swarm optimization was also used by Donelli et al. in the design of a broad-band bidirectional amplifiers [13]. Design of microwave devices by fitness-estimation-based particle swarm optimization algorithm was suggested by Fan et al. [14]. Particle swarm optimization combined with the simulated annealing and extremal optimization algorithms was applied for the solution of the inverse scattering problem for determining the shape and location of perfectly conducting scatterers by Mhamdi [15].

The main motivation in this work was to use particle swarm optimization technique to enable the matching at three distinct frequencies especially for complex loads which is very difficult to attain. As a further contribution, the design was evaluated at measurement level so as to make sure that the values obtained can be realized in real circuits.

The organization of the paper is as follows: in Section II the mathematical analysis for the transmission line transformer modelling is described. In Section III the optimization algorithms and specifically particle swarm optimization is explained. In section IV, the design

procedure and definition of resistive and complex load design is described. In Section V, the simulation results for all three different networks are shown. In Section VI, measurement environment and measured results are presented. In Section VII, concluding remarks are given.

## II. ANALYSIS

A simple n-section transmission line transformer is illustrated in Fig. 1. Simply we can consider an arbitrary load with impedance  $Z_L=R_L+jX_L$  connected to a series of transmission lines with characteristic impedances  $Z_1, Z_2$ , up to  $Z_n$  and with transmission line lengths  $l_1, l_2$ , up to  $l_n$  respectively.

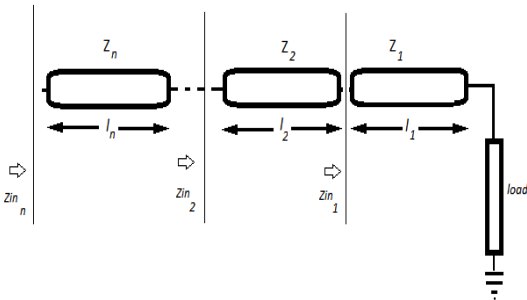


Figure 1. n-section transmission line transformer

Simply using the ideal transmission line theory, we can obtain the intermediate impedances, for example the first impedance becomes:

$$Z_{in_1} = Z_1 \frac{Z_L + jZ_1 \tan(\beta l_1)}{Z_1 + jZ_L \tan(\beta l_1)} \quad (1)$$

where  $\beta$  is the phase constant, similarly extending (1), the second impedance becomes:

$$Z_{in_2} = Z_2 \frac{Z_{in_1} + jZ_2 \tan(\beta l_2)}{Z_2 + jZ_{in_1} \tan(\beta l_2)} \quad (2)$$

and this cascading can be repeated depending on the number of transmission lines used in the design, which means the general formula can be extended as:

$$Z_{in_k} = Z_k \frac{Z_{in_{(k-1)}} + jZ_k \tan(\beta l_k)}{Z_k + jZ_{in_{(k-1)}} \tan(\beta l_k)} \quad (3)$$

where  $k$  indicates the number of section of transmission lines. Naturally a recursion of this calculation is necessary depending on the number of transmission lines.

This also indicates that there will be  $2*k$  variables for  $k$  transmission lines that can be varied. Although this can be a tedious work, this difficulty can be solved when a computer is utilized especially for the recursion process. The addition of a suitable effective evolutionary algorithm as an extra aid, this design process can be efficiently and correctly completed.

Using evolutionary optimization algorithms in the design problems or in finding optimum points became very popular due to the advancement of computer programming. If we consider some recent work: optimization based on phylogram analysis and composed exhaustive search were developed to find solutions for combinatorial optimization

problems with different levels of difficulty by Soares et al. [16]. Purcaru et al. used another evolutionary algorithm called gravitational search algorithm to find optimal robot path [17]. Finding new optimization algorithms or modifying existing algorithms for improvement is also popular in order to find more efficient methods in optimization and design problems. Recently Naseri and Hasheminejad suggested a different gene selection method on multi-objective ant colony optimization [18]. New methods and algorithms arise frequently. Some of the new algorithms that can be listed: ideal gas optimization algorithm [19], modified version of cuckoo search, island-based cuckoo search [20], grey wolf optimizer [21], Harris Hawks optimization [22], and crossover optimization [23].

Knowing the usefulness of optimization algorithms and combining the previous problem, we can simply consider equation (3), which is a recursive function model with  $2*k$  unknowns as indicated, as our optimization problem. It is a recursive function, and in order to determine the unknown values (impedances and lengths) we can apply an evolutionary algorithm.

## III. PARTICLE SWARM OPTIMIZATION

Particle swarm optimization is an algorithm which was originally developed by Eberhart and Kennedy [24]. After its emergence, it got the attention of many researchers in many different ways. For example, researchers and computer scientists worked on the improvement of the algorithm. Dynamically adapting the inertia weight using a fuzzy system was one of the earliest modifications to the particle swarm optimization by Shi and Eberhart [25]. Hybrid approach incorporating chaos into particle swarm optimization was suggested by Liu et al. [26]. Incorporating aging leader and challengers into particle swarm optimization was proposed by Chen et al. [27]. Addition of differential evolution mutation operator to the accelerated particle swarm optimization was proposed by Wang et al. [28]. Yang et al. proposed self-adaptive inertia weight to speed up the convergence rate recently [29]. For data clustering improved hybrid method based on cuckoo optimization and modified particle swarm optimization was suggested by Bouyer and Hatamlou [30]. Anand and Suganti suggested the use of hybrid genetic algorithm and particle swarm optimization for forecasting electricity demand [31]. Ulker proposed combining significant properties of particle swarm optimization and harmony search algorithm forming a hybrid algorithm and verified the performance with two optimization problems [32].

Some researchers worked on the application of this algorithm to different problems. Wang et al. proposed the application of the particle swarm optimization algorithm to the travelling salesman problem using the swap operator and swap sequence [33]. Recently Pijarski and Kacejko used particle swarm optimization in the optimization of voltage levels and reactive power flows which were related to reactive power compensation [34]. Nammalvar and Ramkumar used parameter improved particle swarm optimization for enhancing system performance and stability in the integration of photovoltaic array in an AC micro-grid [35]. Fu et al. used particle swarm optimization in big data digging as an application [36]. Chih solved multi-

dimensional knapsack problem using a modified version of particle swarm optimization [37]. A maritime industry application as a collision risk assessment, particle swarm optimization algorithm was used by Inan and Baba to find the safe and shortest path for avoiding the collision [38]. Especially in electromagnetic theory and microwave engineering the topic has found many different applications. Robinson and Rahmat Samii was one of the first in the electromagnetics area to use the particle swarm optimization technique [39]. Ulker designed simple matching network and a coupler using solely particle swarm optimization technique [40], also the work was extended to different multi-objective problems with different microwave circuit configurations [41-43].

In its simple explanatory form, the algorithm uses particles (e.g. birds) which are placed in the search space randomly and they move around the search space until the search criterion is met. Each particle uses its own history and also the location of the best particle (i.e. leader) to reach to the final desired solution. The algorithm in its basic original version is shown in Fig. 2. In the figure,  $v[i]$  and  $present[i]$  indicate the velocity and position vectors, where  $i$  represent the index of a particle.  $w$  is the inertia weight usually taken between 0.4 to 0.6,  $c_1$  and  $c_2$  are cognition factor and social factor constants usually taken to be close to the value 2. The parameter  $rand()$  adds randomness to the velocity equation. Usually this parameter improves the exploration in the space of interest and exploitation, while at the same time prevents premature convergence to a local optimum point [44,45].

```

Step 1. Initialize the particles
Step 2. Do for all the particles
  - Calculate the fitness value for each particle
  - If the fitness value is better than the particles best fitness value (pbest) in history set the current value as the new pbest
Step 3. Find the best particle with the smallest fitness value after comparing with all the particles and set that one as the global best (gbest)
Step 4. Calculate and update each particles velocity and position using:
   $v[i]=w*v[i]+c_1*rand()* (pbest[i]-present[i])+c_2*rand()* (gbest-present[i])$ 
   $present[i]=present[i]+v[i]$ 
Step 5. Calculate the fitness value for each particle
Step 6. Repeat steps 2-5 until the minimum error criterion is met

```

Figure 2. Basic steps of particle swarm optimization

Simply the algorithm can be applied to any research problem which the model can be constructed. The research problem can be more challenging if the problem has a multi-objective nature. However, there are many cases which this multi-objective criterion was tackled successfully as some approaches were for the application and some approaches were for developing different strategies.

Although most of the multi-objective particle swarm optimization algorithms adopt single search strategy while updating the velocity vector, Lin et al. proposed a multi-objective particle swarm optimization using multiple search strategies [46]. Ma and Qu used multi-objective particle swarm optimization in the design optimization of switched reluctance motors as maximizing torque per active mass, maximizing efficiency and minimizing torque ripple [47]. Duchaud et al. used multi-objective particle swarm optimization in optimal sizing of a renewable hybrid power plant in reducing the annualized cost of the system and the imported energy without failing to supply the load [48].

Recently geographic information system based multi-objective particle swarm optimization of charging stations for electric vehicles as minimizing the total costs and maximizing the coverage was suggested by Zhang et al. [49]. As indicated previously, we can consider equation (3) in a recursive fashion yielding to five unknowns in resistive load designs and yielding to six unknowns in complex load design. These are the unknowns that need to be found and optimized. The difficulty here is finding the optimum values that satisfy the resonance at three different frequencies. In a way the problem becomes a multi-objective optimization problem.

In this work the particle swarm optimization algorithm is applied for this multi-objective optimization problem. First analysis of optimization constants was done. After some preliminary evaluations of the algorithm were completed, the number of particles was set to 20. The inertia weight  $w$  was set to 0.4 and the cognition and social factor constants,  $c_1$  and  $c_2$ , were set to 1.99. The number of iterations was limited to 20000. From the preliminary evaluations, this number was enough for finding suitable solutions for this problem.

#### IV. DESIGN PROCEDURE

The design process essentially relies on using the equation (3) as our fitness equation and using the particle swarm optimization technique to solve for the variables under question. The steps for the design procedure can be outlined in Fig. 3, when the below algorithm completes, the program output directly produces the design parameter values.

```

Step 1. Initialize the 20 particles with each holding the unknown variables
Step 2. Do for all the particles:
  - Calculate the fitness value for center frequency
  - Calculate the fitness value for lower frequency
  - Calculate the fitness value for higher frequency
Step 3. Find the best particle with smallest fitness value and set that one as global best
Step 4. Calculate and update each particles velocity and position
Step 5. Repeat the steps 2,3,4 until overall fitness value is zero (or close to zero) or until the number of iterations reach to 20000

```

Figure 3. Steps of designing for tri-band impedance matching network

In order to test this design process, two different load types were considered. One of the load type was for real load of impedances  $100\Omega$  and  $200\Omega$ . The second load type was for a complex load of impedance  $100\Omega$  in parallel with a  $1\text{ pF}$  capacitor.

##### A. Resistive Load Design ( $100\Omega$ and $200\Omega$ )

In this work for the first load type, a resistive load of  $100\Omega$  and in the second a resistive load of  $200\Omega$  were used. In these cases automatically we set all the transmission line lengths to  $\lambda/4$ , making the problem a multi-section quarter wave transformer problem. All of the five unknowns are the characteristic impedances of the transmission lines,  $Z_1, Z_2, Z_3, Z_4, Z_5$ . So these impedances were used in the objective function as the optimizing variables. The range was restricted for these values in the algorithm as  $10\Omega \leq Z_k \leq 135\Omega$ . The triple band resonant frequencies were selected to be 1.8 GHz, 2.4 GHz, and 3.0 GHz.

### B. Complex Load Design (100Ω in Parallel with 1 pF Capacitor)

In the second load type, the load was chosen as a complex load of 100Ω in parallel with a 1pF capacitor. In this case automatically we set all the lengths except for the first one (transmission line attached to the load) to  $\lambda/4$ . The first length  $l_1$  was set as a random variable which needed to be optimized together with the impedances. In other words, the six unknowns were the characteristic impedances of the transmission lines,  $Z_1, Z_2, Z_3, Z_4, Z_5$  and the length  $l_1$ . So these impedances and the length value were used in the objective function as the variables which needed to be determined and optimized. The range was restricted for these values in the algorithm as  $10\Omega \leq Z_k \leq 120\Omega$  and the length value was set to be in the range 0-1λ. The frequencies for optimization were selected to be again 1.8 GHz, 2.4 GHz and 3.0 GHz.

## V. SIMULATION RESULTS

The multi-objective particle swarm optimization program was written in C++ language using a desktop computer with Intel i5 processor and 4 GB RAM. The separate tables were obtained for all different networks. In the tables,  $Z_k$ 's indicate the impedance values. 'First Conv.' represents how many iterations passed for the first particle to reach to an optimum solution whereas 'Final' represents after 20000 evaluations the number of particles reaching to a solution (out of 20).

The fitness values were checked to see the closeness of the answers to the desired matching impedance value of 50Ω. Six variables were defined for this purpose. 'fit' is the variable that was used to check the impedance value's real part at the end of the matching network at the design value of 2.4 GHz. 'fit 1' is the variable that was used to check the impedance value's imaginary part at the end of the matching network at the design value of 2.4 GHz. 'fit 2' is the variable that was used to check the impedance value's real part at the end of the matching network at the design value of 1.8 GHz. 'fit 3' is the variable that was used to check the impedance value's imaginary part at the end of the matching network at the design value of 1.8 GHz. 'fit 4' is the variable that was used to check the impedance value's real part at the end of the matching network at the design value of 3.0 GHz. 'fit 5' is the variable that was used to check the impedance value's imaginary part at the end of the matching network at the design value of 3.0 GHz.

### A. Network 1 (100Ω Load)

For this network some of the obtained design values are tabulated in Table I. Fitness values being close to 0 indicates the success of the algorithm.

All the impedance values in the solution were in between 40Ω to 95Ω. The fitness values, which indicated the closeness of the correct impedances to have matching at three design frequencies, were all very low as expected. Ideally for a perfect match we should have observed the 0 value as fitness value. In some cases this was observed, in the other fitness values, although these values were not exactly 0, they were very close to 0. This showed that the design values obtained using the algorithm lead to a satisfactory solution.

Moreover, it was observed that the number of iterations for finding a suitable solution was very low. Even when the iterations of about 50 were reached, the first particles were producing a fitness value almost as close to 0. In other words, particles producing these low fitness values were in the vicinity of a possible optimized solution. Having such a low number of iterations for particles reaching to a proper solution can be accounted because of the simplicity of the problem, having a purely resistive load to match. Also another observation that could be made is the fact that at least 17 out of 20 particles reach to the optimum solution in 20000 evaluations. Further analysis for a sample of results was performed. Fig. 4 shows the number of particles out of 20 reaching to a solution as the iterations progresses. As it can be seen even at about 250 iterations all the particles are within the limits of finding a solution. A second analysis was done for observing how small the overall fitness value gets as the number of iterations progresses. It can be seen in Fig. 5 that, as early as in 30 iterations the fitness value is below 0.5, at about 100 iterations the value for overall fitness is below 0.2. Furthermore, at about 140 iterations the overall fitness value drops to zero.

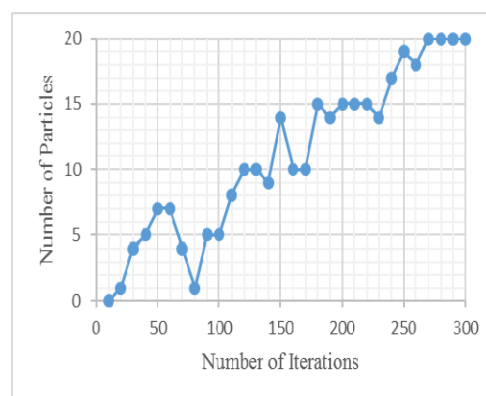


Figure 4. Particles reaching to an optimum solution for Network 1

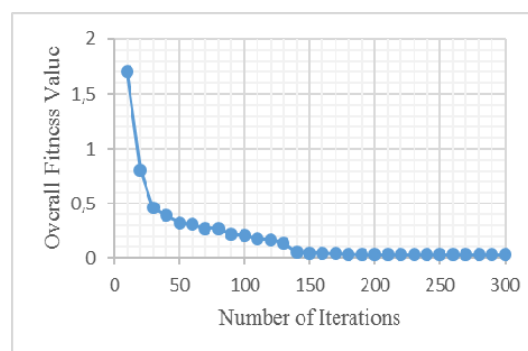


Figure 5. Overall fitness value as the iteration progresses for Network 1

The performance of the algorithm can not be compared exactly with other work since the circuit structure used in this case was unique. However the best comparable paper related with this work is Khodier et al.'s work [4]. In one of their analysis, they designed quad-band four section transmission line transformer. Their best values with 20 particles were around 200 iterations for reaching to an acceptable level of fitness. In our case this value was about 140 iterations.

TABLE I. SAMPLE OUTPUT RESULTS FROM PARTICLE SWARM OPTIMIZATION FOR 100Ω DESIGN

$Z_1$ (Ω)	$Z_2$ (Ω)	$Z_3$ (Ω)	$Z_4$ (Ω)	$Z_5$ (Ω)	fit	fit 1	fit 2	fit 3	fit 4	fit 5	First Conv.	Final
93.72	78.00	62.12	53.59	50.76	0.000305	0.00004	0.00009	0.30075	0.173157	0.000303	90	17
92.20	68.04	46.38	40.62	45.70	0	0.00006	0.980095	0	0.000954	0.394029	50	17
89.58	72.61	61	56.16	52.76	0	0.00016	0	0.348560	1.133392	0.00068	50	20
90.07	67.30	49.95	45.74	48.38	0.000004	0.00002	0.000019	0.544603	0.000763	0.184147	60	20
92.65	79.25	66.99	58.56	52.87	0	0.00012	0	0.129573	0.833904	0.000002	60	20

The set of impedance values:  $Z_1=80.22\Omega$ ,  $Z_2=63.86\Omega$ ,  $Z_3=64.93\Omega$ ,  $Z_4=69.68\Omega$ ,  $Z_5=60.38\Omega$  were used in a microwave simulator to see whether the obtained impedance values produced the desired triple band performance. The microwave simulator used was PUFF [50]. The simulation response is shown in Fig. 6.

In Fig. 6, we can clearly see that the three resonances occurred at the desired frequencies. Also it can be seen that resonances are sharp. At 1.8 GHz and 3 GHz the resonances are both below -25 dB and at 2.4 GHz the matching is even better with a value of below -30 dB. These sharp resonances are direct indication of fitness values both real and imaginary all being close to 0 and at all three frequencies.

In this case it is worthwhile to mention that the problem at hand is relatively easy problem with resistive load and five unknowns to be determined compared to complex load problems which needs six unknowns to be determined. As a result in the simulations, all the runs produced convergences to an answer. Furthermore this convergence occurred very fast and produced very reliable design impedance values.

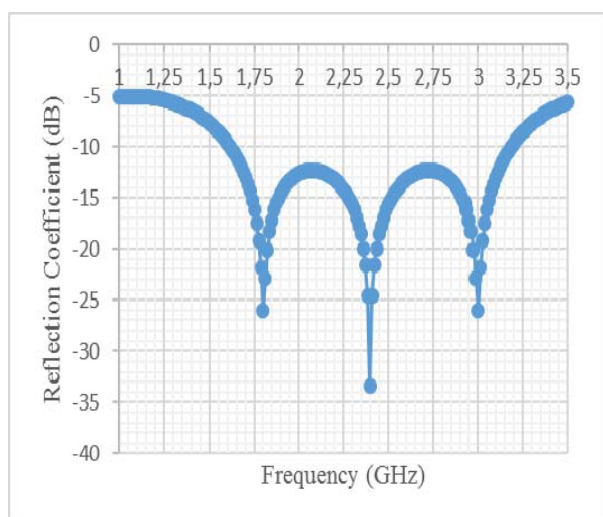


Figure 6. Simulation reflection coefficient vs. frequency for Network 1

### B. Network 2 (200Ω Load)

For this problem some answers which were obtained is tabulated in Table II. Here the main solutions were also observed to be in between  $20\Omega$  to  $135\Omega$  for the impedances. The fitness values were again very low. Specifically the center frequency for matching, which was 2.4 GHz, all the fitness values observed were lower than  $1 \times 10^{-3}$ . Some deviations from the value 0 occurred especially for the fitness values which were used to check the matching value at 1.8 GHz and 3 GHz. In the matching for 1.8 GHz,

especially the imaginary part indicated some possible deviations from the value 0. For the 3 GHz matching, sometimes both the real part and the imaginary part of the impedance showed the slight deviations from the value 0. However, when the overall solutions were analyzed, this was not very crucial.

Also the convergence to the optimum value was very fast, similar to the previous network and the number of particles reaching to the solution was usually very high. This was again due to the fact that the load that was used in this analysis was a resistive load. In this case further analysis for seeing the number of particles reaching to an acceptable solution with number of iterations is shown in Fig. 7 for a sample run.

Again we see that couple of particles reach to an optimum solution in about 100 iterations and by 400 iterations almost half of the particles have already reached to a reasonable solution. In the second analysis, as shown in Fig. 8, we observe the overall fitness value as the number of iterations progresses. We see that after about 100 iterations overall fitness value reaches to a value less than 1.

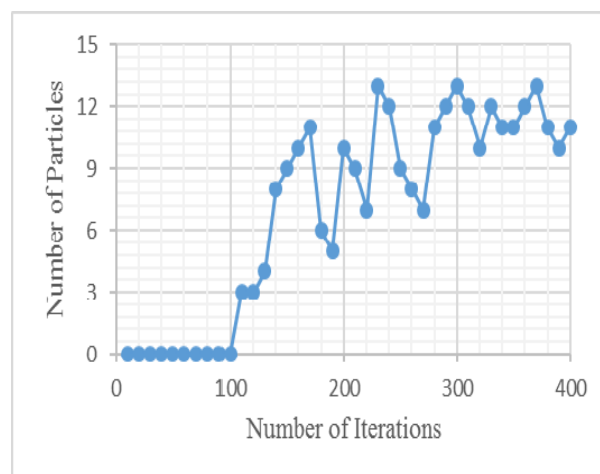


Figure 7. Particles reaching to an optimum solution for Network 2

We selected a set of values to test on a microwave simulator PUFF again. The set that is used has the following impedance values:  $Z_1=101.78\Omega$ ,  $Z_2=49.76\Omega$ ,  $Z_3=55.66\Omega$ ,  $Z_4=92.71\Omega$ ,  $Z_5=81.44\Omega$ . The obtained response is shown in Fig. 9. As before the simulation indicated one big resonance going down to -40 dB at the center design frequency and two relatively smaller resonances at 1.8 GHz and 3 GHz with values about -15 dB.

TABLE II. SAMPLE OUTPUT RESULTS FROM PARTICLE SWARM OPTIMIZATION FOR 200Ω DESIGN

Z <sub>1</sub> (Ω)	Z <sub>2</sub> (Ω)	Z <sub>3</sub> (Ω)	Z <sub>4</sub> (Ω)	Z <sub>5</sub> (Ω)	fit	fit 1	fit 2	fit 3	fit 4	fit 5	First Conv.	Final
131	55.37	29.97	32.43	45.74	0.000004	0.000042	0.000004	0.000486	2.899490	2.610447	170	18
131	49.97	23.12	24.53	40.44	0.000004	0.000023	0.000008	0.006542	1.175072	3.198831	290	20
131	58.50	85.14	41.47	51.65	0.000271	0.000056	0.000092	2.915597	3.533730	0.106775	90	12
103.6	49.81	52.91	86.13	78.31	0	0.000168	0.000015	3.370557	13.381416	0.000002	50	20
129.8	64.47	46.90	54.95	58.22	0	0.000075	0.000011	2.253299	5.365112	0.000027	60	20

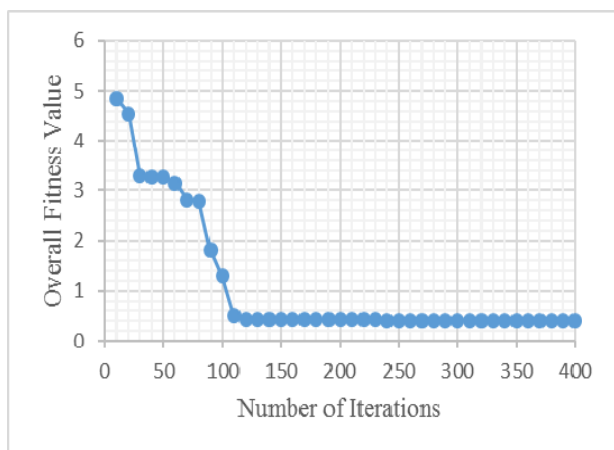


Figure 8. Overall fitness value as the iteration progresses for Network 2

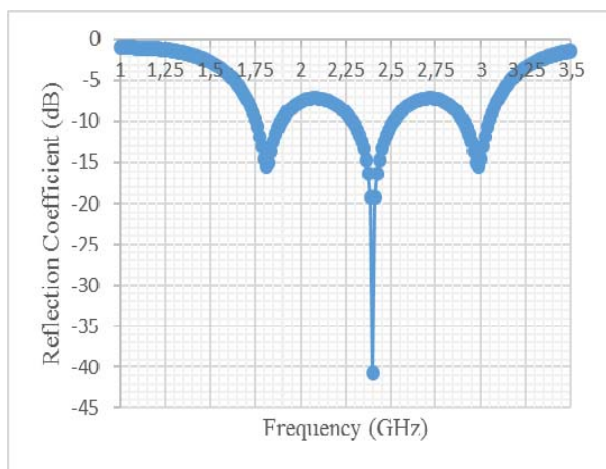


Figure 9. Simulation reflection coefficient vs. frequency for Network 2

C. Network 3 (100Ω Parallel with 1 pF Capacitor Load)

For this problem some possible solutions which are obtained by running the program is tabulated in Table III. In this case there were six variables as explained before, which affected the convergence to a solution. Also since the algorithm was run under the same conditions as constants being the same, it required more number of iterations for reaching to a solution.

Fitness values however were very low which showed a success in finding an optimum solution to the problem at hand. Also these numbers being very close to the value 0 shows us that in fact the solution quality of the impedance values and length value found are very good. Analysis of results for observing the convergence for a sample output was done and it is shown in Fig. 10 and Fig. 11. As shown

in Fig. 10, the first particle reaching to a convergence in this sample set was after about 3500 iterations. Although we would like to point out that depending on different solution sets, the number of iterations may differ as it can be observed in Table III. When the results are compared we see that about 8 particles are within the boundaries of a correct solution in about 4000 iterations. Also when Fig. 11 is analyzed, we see that as the number of iterations increase, overall fitness value keeps getting closer to 0 as expected, in this sample set the drops start after around 3000 iterations.

It is worthwhile to mention that especially the convergence rate is affected with the type of load. In Network 3, since the load type is complex, the convergence rate is slower compared to the other Networks (Network 1 and Network 2). However, it is important to realize that the solution quality is as good as the previous cases. In another words the different load type is not affecting the solution quality drastically but seemed to be having an observable effect on the convergence rate.

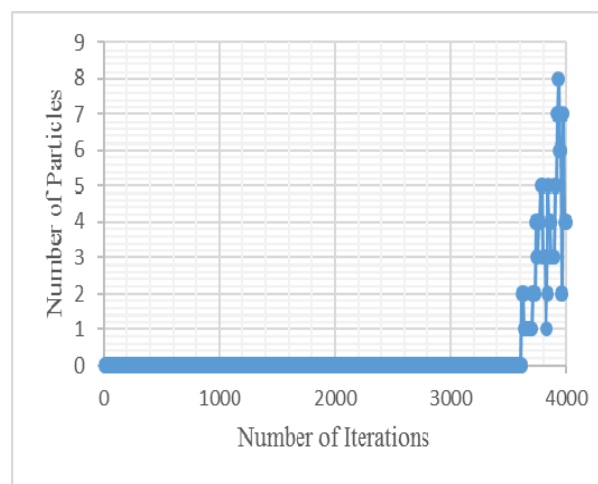


Figure 10. Particles reaching to an optimum solution for Network 3

One set of data is used to test the obtained impedances and transmission line length on microwave simulator. The set that is used has the following impedance values: Z<sub>1</sub>=35.09Ω, Z<sub>2</sub>=79.96Ω, Z<sub>3</sub>=62.85Ω, Z<sub>4</sub>=20.93Ω, Z<sub>5</sub>=16.46Ω and the transmission line length value is 0.415865λ (149.71°). The obtained simulation response using this set is shown in Fig. 12. Again one clear dip at the resonant frequency of 2.4 GHz is seen reaching down to -35 dB and the two side resonances occurring at frequencies of 1.8 GHz and 3 GHz as about -15 dB and -9 dB respectively.

TABLE III. SAMPLE OUTPUT RESULTS FROM PARTICLE SWARM OPTIMIZATION FOR 100Ω PARALLEL WITH 1 PF CAPACITOR DESIGN

$Z_1$ (Ω)	$Z_2$ (Ω)	$Z_3$ (Ω)	$Z_4$ (Ω)	$Z_5$ (Ω)	$I_1$ (A)	fit	fit 1	fit 2	fit 3	fit 4	fit 5	First Conv.	Final
52.65	108.9	70.94	22.37	18.36	0.379615	0.00008	0.00005	0.00008	0.00003	0.01153	0.00008	1010	7
68.67	72.54	50.71	23.30	15.40	0.854545	0.00026	0.00011	0.09014	0.31658	0.09023	0.00026	770	12
78.57	79.85	51.12	21.86	14.43	0.842611	0.00013	0.00166	0.00045	0.00090	0.00171	0.00020	960	7
68.90	71.67	49.01	22.41	15.11	0.854241	0.00021	0.00078	0.00066	0.00068	0.00024	0.00049	1970	9
35.09	79.96	62.85	20.93	16.46	0.415865	0.00057	0.00059	0.00078	0.00216	0.00016	0.00012	1140	10

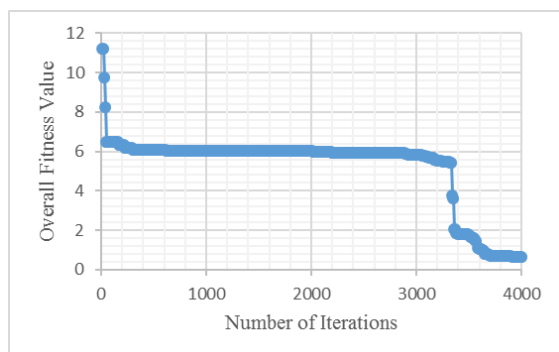


Figure 11. Overall fitness value as the iteration progresses for Network 3

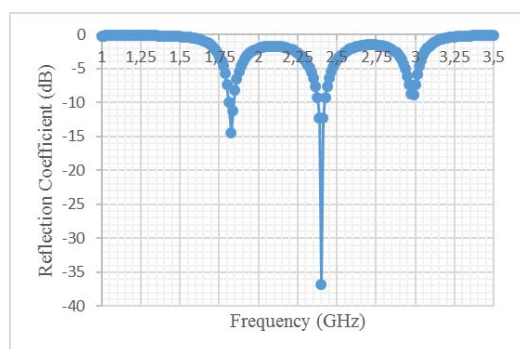


Figure 12. Simulation reflection coefficient vs. frequency for Network 3

## VI. MEASUREMENT RESULTS

The responses that were obtained from the algorithm were tested by the simulators as shown in the previous section but further verification was necessary. As a consequence, the implementation of these circuits by fabricating them on Rogers Dielectric RO6010.2 substrate [51] with thickness 1.27 mm and dielectric constant of 10.2 was done. We had a capacitor of 1.2 pF available so rather than 1 pF, 1.2 pF capacitor was assembled for Network 3. RF ground was realized using an open circuited quarter wave transformer for all the circuits.

The picture of the circuits for Network 1 (100Ω load) and Network 2 (200 Ω load) are shown in Fig. 13, and for Network 3 (100 Ω parallel with 1.2pF capacitor load) in Fig. 14. The circuits were then tested with Vector Network Analyzer PXIe-6532 from National Instruments [52]. The measurement results together with simulation results for each of the three cases are presented in Fig. 15, Fig. 16 and Fig. 17 for the cases of 100 Ω load, 200 Ω load, 100 Ω and 1.2pF parallel capacitor load respectively.

When we analyze the circuit for Network 1, we see that the dip at 0.5 GHz was also occurring in both the simulation and measurement. One of the design frequencies was 1.8 GHz and it was noticed that this occurred both in simulation

and in measurement to be at 1.785 GHz as -14.716 dB in measurement, and as -16.576 dB in simulation.



Figure 13. Photograph for Network 1 and Network 2

In the simulation, the second design frequency which was set as 2.4 GHz occurred at 2.38 GHz as -23.768 dB and in measurement this occurred at a shifted frequency 2.593 GHz as -8.608 dB. The third design frequency which was set as 3 GHz occurred at 3.018 GHz in simulation, however this dip shifted in this circuit to 3.485 GHz and it was not very low, only -5.697 dB. The mismatches were probably due to fabrication errors as well as mismatch between the connectors and circuits.

When we compare the simulated and measured responses for Network 2, we see that roughly the expected behavior was observed. The dip at 0.383 GHz in simulation as -4.267 dB occurred at the same frequency but as -2.496 dB. The first design frequency occurred at 1.827 GHz in simulation and as -13.665 dB. On the other hand, in measurements this occurred at 1.743 GHz and as -12.961 dB. The second design frequency occurred at 2.380 GHz as -17.447 dB however in measurement this dip in frequency was shifted to 2.295 GHz as -5.955 dB.

The third design frequency occurred at 2.975 GHz as -13.767dB, the measurement also indicated this dip however the value was -5.607 dB.

For the circuit in Network 3, the simulation was done again for the modified version of using 1.2 pF rather than 1 pF. As we can observe Fig. 12 and Fig. 17 we see that the responses in terms of design frequencies do not vary drastically when frequency operating points are considered.

In Figure 17, when we compare the responses we see that there was a low frequency dip occurring at 0.51 GHz as -8.425dB which was also occurring at the same frequency in measurement at a lower value -4.688 dB.



Figure 14. Photograph for Network 3

The first design frequency of 1.8 GHz occurred at 1.828 GHz as -10.044 dB and also the similar observation took place for measurement but only at -0.836 dB. The second design frequency occurred at 2.38 GHz at -12.076 dB in simulation and for measurement at the same frequency -5.383 dB.

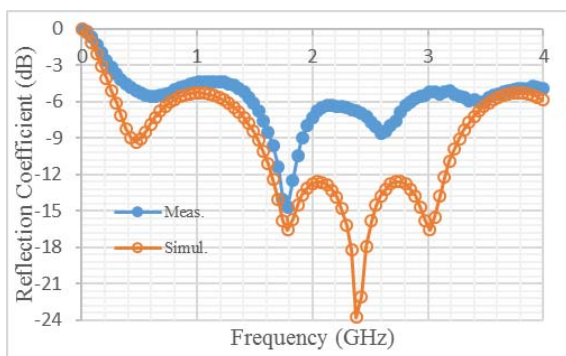


Figure 15. Simulated and measured response for Network 1 (100 Ω load).

The third design frequency occurred at 2.975 GHz -5.088 dB for the simulation and at 2.848 GHz as -2.818 dB for the measurement. Also another dip was observed in measurement at 3.783 GHz as -6.058 dB. It is important to note that although some of the design frequencies did not exhibit significant resonances, they were all observable at their designed operating frequencies.

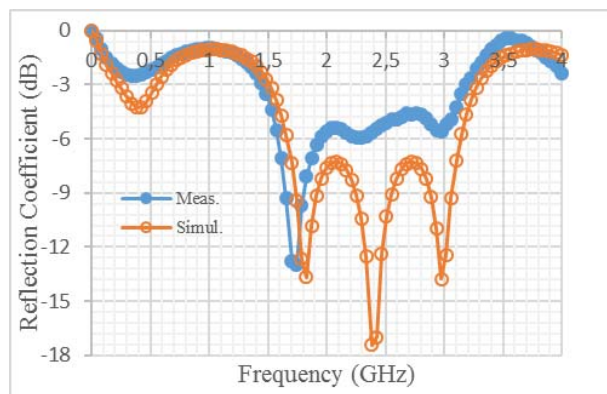


Figure 16. Simulated and measured response for Network 2 (200 Ω load)

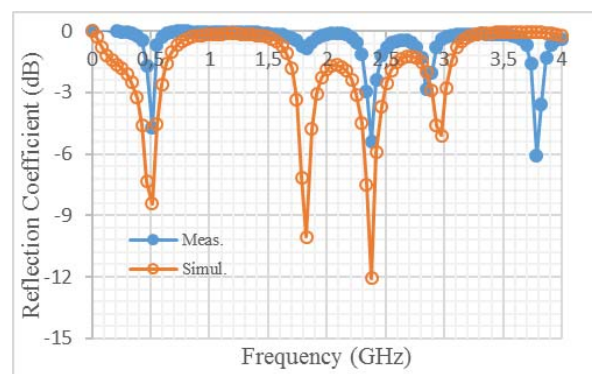


Figure 17. Simulated and measured response for Network 3 (100 Ω parallel to 1.2 pF circuit)

## VII. CONCLUSIONS

In this work the design of five section impedance transformer is presented which the design values are obtained and optimized by particle swarm optimization algorithm. The transformer in this case was for matching at three different frequencies. The proposed design procedure can be easily extended by adding extra transmission lines with various impedances and lengths, and increasing the unknown variables accordingly. In this work, the tests were performed at the frequencies of 1.8 GHz, 2.4 GHz and 3 GHz. The optimized impedance and length design values, obtained by the particle swarm optimization which simultaneously satisfies the resonance condition at these three different frequencies, were verified by simulators.

The circuits were fabricated to further validate the design values obtained by the optimization algorithm. The measurements were taken accordingly and three frequency dips were all observed in all of the designs although the distinction was not very clear in some designs. However, it can be deduced that in fact multiple section transformer networks can be designed and effectively optimized using particle swarm optimization technique.

Further work can be conducted by adding various more vigorous constraints to the algorithm to make sure that the dips are clear and all well below -20 dB at the simulation stage. Also, the parameters of the algorithm can be tuned further for obtaining the simulation responses better. This is going to be very useful because some of the resonances are barely showing themselves in the response. This would hopefully make the resonances sharper especially in Network 3 which the load is complex. In the design and fabrication stage, using different dielectric substrates may lead to a more accurate match between the simulation and

real circuit responses. While taking the measurements also extra precaution can be added to make sure the connections are done properly as well as adding via holes as ground rather than using  $\lambda/4$  long open circuited transmission lines as ground.

## ACKNOWLEDGEMENT

The author wishes to thank to Christopher Moore and Professor Dr. Robert M. Weikle from the Electrical and Computer Engineering Department of University of Virginia, United States for their help in the fabrication and measurements stage of the project. Author also wishes to thank Assoc. Prof. Dr. Ezgi Deniz Ülker from Computer Engineering Department, European University of Lefke, Turkey, for her help in programming stage and discussion about the performance of the algorithm as well as suggestions for improving the performance of the algorithm and making it robust.

The author also wishes to thank the reviewers of this work and manuscript who contributed to the development of this paper to better standards.

## REFERENCES

- [1] M. Chongcheawchamnan, S. Patisang, S. Srisathit, R. Phromloungsri, S. Bunnjaweht, "Analysis and design of a three-section transmission-line transformer," *IEEE Trans. Microwave Theory and Techniques*, vol. 53, issue-7, pp. 2458-2462, July 2005. doi:10.1109/TMTT.2005.850408
- [2] X. H. Wang, L. Zhang, Y. Xu, Y. F. Bai, C. Liu, X.-W. Shi, "A tri-band impedance transformer using stubbed coupling line," *Progress in Electromagnetics Research*, vol.141, pp. 33-45, 2013. doi: 10.2528/PIER13042907
- [3] Z. Hu, C. Huang, S. He, F. You, "Tri-band matching technique based on characteristic impedance transformers for concurrent tri-band power amplifiers design," in *TENCON 2015- 2015 IEEE Region 10 Conference*, 1-4 Nov. 2015. doi: 10.1109/TENCON.2015.7373074
- [4] M. Khodier, N. Dib, J. Ababneh, "Design of multi-band multi-section transmission line transformer using particle swarm optimization," *Electrical Engineering*, vol. 90, issue 4, pp. 293-300, April 2008. doi: 10.1007/s00202-007-0077-z
- [5] L. -C. Tsai, "Design of triple-band impedance transformers using Z-transform techniques," *IEEE Microwave and Wireless Component Letters*, vol. 26, issue: 8, pp. 559-561, August 2016. doi:10.1109/LMWC.2016.2585542
- [6] L. -C. Tsai, "Triple-band impedance transformers using equal-length serial transmission lines," *IET Microwaves, Antennas & Propagation*, vol. 10, issue 5, pp. 568-573, April 2016. doi: 10.1049/iet-map.2015.0633
- [7] J. Kim, Y. Lee, "A Z-transform method for synthesis of unequal-length multisection transmission lines for multiband applications," *IEEE Transactions on Microwave Theory and Techniques*, vol. 65, issue:9, pp. 3200-3210, September 2017. doi: 10.1109/TMTT.2017.2678474
- [8] Y. Li, T. Cantin, B. Derat, D. Pasquet, J.-C. Bolomey, "Application of resonant matching circuits for simultaneously enhancing the bandwidths of multi-band mobile phones," in *2007 International Workshop on Antenna Technology: Small and Smart Antennas Metamaterials and Applications*, pp. 479-482, June 2007. doi: 10.1109/IWAT.2007.370178
- [9] G. Sami, M. Mohanna, M. L. Rabeh, "Tri-band microstrip antenna design for wireless communication applications," *NRIAG Journal of Astronomy and Geophysics*, 2, pp. 39-44, (2013). doi: 10.1016/j.nrjag.2013.06.007
- [10] M. Chongcheawchamnan, S. Patisang, M. Krairiksh, I.D. Robertson, "Tri-band Wilkinson power divider using a three-section transmission-line transformer," *IEEE Microwave and Wireless Components Letters*, vol. 16, issue 8, pp. 452-454, August 2006. doi: 10.1109/LMWC.2006.879488
- [11] N. Dib, M. Khodier, "Design and optimization of multi-band Wilkinson power divider," *International Journal of RF and Microwave Computer-Aided Engineering*, vol. 18, Issue 1, pp. 14-20, January 2008. doi: 10.1002/mmce.20261
- [12] X.-f. Luo, "Differential evolution strategy cum equivalent circuit method for the design of multi-band frequency selective surfaces," *The Journal of China Universities of Posts and Telecommunications*, vol. 18, supp. 1, pp. 101-105, September 2011. doi: 10.1016/S1005-8885(10)60202-6
- [13] M. Donelli, Md. Rukanuzzaman, C. Saavedra, "A methodology for the design of microwave systems and circuits using an evolutionary algorithm," *Progress in Electromagnetics Research M*, vol. 31, pp. 129-141, 2013. doi: 10.2528/PIERM13041607
- [14] X.-h. Fan, Y.-b. Tan, Y. Zhao, "Optimal design of microwave devices by fitness estimation-based particle swarm optimization algorithm," *Applied Computational Electromagnetics Society Journal*, vol.33, no. 11, pp. 1259-1267, Nov. 2018.
- [15] B. Mhamdi, "Microwave imaging based on two hybrid particle swarm optimization approaches," *International Journal of Microwave and Wireless Technologies*, vol. 11, issue 3, pp. 268-275, April 2019. doi:10.1017/S1759078718001484
- [16] A. Soares, R. Rabelo, A. Delbem, "Optimization based on phylogram analysis," *Expert Systems with Applications*, vol. 78, pp. 32-50, July 2017. doi: 10.1016/j.eswa.2017.02.012
- [17] C. Purcaru, R.-E. Precup, D. Iercan, L.-O. Federovici, R.-C. David, F. Dragan, "Optimal robot path planning using gravitational search algorithm," *International Journal of Artificial Intelligence*, vol. 10, no: S13, pp. 1-20, March 2013.
- [18] A. Naseri, S. M. H. Hasheminejad, "An unsupervised gene selection method based on multiobjective ant colony optimization," *International Journal of Artificial Intelligence*, vol. 17, no: 2, pp. 1-22, October 2019.
- [19] M. Shams, E. Rashedi, S. M. Dashti, A. Hakimi, "Ideal gas optimization algorithm," *International Journal of Artificial Intelligence*, vol. 15, no. 2, pp. 116-130, October 2017.
- [20] B. H. Abed-alguni, "Island-based cuckoo search with highly disruptive polynomial mutation," *International Journal of Artificial Intelligence*, vol. 17, no. 1, pp. 57-82, March 2019.
- [21] S. Mirjalili, S. M. Mirjalili, A. Lewis, "Grey wolf optimizer," *Advances in Engineering Software*, vol. 69, pp. 46-61, March 2014. doi: 10.1016/j.advengsoft.2013.12.007
- [22] A. Heidari, S. Mirjalili, H. Faris, I. Aljarah, M. Mafarja, H. Chen, "Harris hawks optimization: algorithm and applications," *Future Generation Computer Systems*, vol. 97, pp. 849-872, August 2019. doi: 10.1016/j.future.2019.02.028
- [23] P. Mei, L. Wu, H. Zhang, Z. Liu, "A hybrid multi-objective crisscross optimization for dynamic economic/emission dispatch considering plug-in electric vehicles penetration," *Energies*, vol. 12, issue 20, 3847, October 2019. doi: 10.3390/en12203847
- [24] R. Eberhart, J. Kennedy, "A new optimizer using particle swarm optimization," in *Proceedings of the Sixth International Symposium Micro Machine Human Science*, 4-6 October 1995. doi: 10.1109/MHS.1995.494215
- [25] Y. Shi, R. C. Eberhart, "Fuzzy adaptive particle swarm optimization," in *Congress on Evolutionary Computation*, 27-30 May 2001, pp.101-106. doi: 10.1109/CEC.2001.934377.
- [26] B. Liu, L. Wang, Y.-H. Jin, F. Tang, D.-X. Huang, "Improved particle swarm optimization combined with chaos," *Chaos, Solitons & Fractals*, vol. 25, issue 5, pp. 1261-1271 September 2005. doi: 10.1016/j.chaos.2004.11.095
- [27] W. -N. Chen, J. Zhang, Y. Lin, N. Chen, Z.-H. Zhan, H. S. -H. Chung, Y. Li, Y. -H. Shi, "Particle swarm optimization with an aging leader and challengers," *IEEE Transactions on Evolutionary Computation*, vol. 17, issue:2, pp. 241-258, April 2013. doi: 10.1109/TEVC.2011.2173577
- [28] G. -G. Wang, A. H. Gandomi, X. -S. Yang, A. H. Alavi, "A novel improved accelerated particle swarm optimization algorithm for global optimization," *Engineering Computations*, vol. 31, issue:7, pp.1198-1220, 2014. doi:10.1108/EC-10-2012-0232
- [29] Q. Yang, J. Tian, W. Si, "An improved particle swarm optimization based on difference equation analysis," *Journal of Differential Equation Applications*, vol. 23, issue: 1-2, pp. 135-152, 2017. doi: 10.1080/10236198.2016.1199691
- [30] A. Bouyer, A.Hatamlou, "An efficient hybrid clustering method based on improved cuckoo optimization and modified particle swarm optimization algorithms," *Applied Soft Computing*, vol. 67, pp. 172-182, 2018. doi:10.1016/j.asoc.2018.03.011
- [31] A. Anand, L. Suganthi, "Hybrid GA-PSO optimization of artificial neural network for forecasting electricity demand," *Energies*, vol. 11(4), 728, 2018. doi: 10.3390/en11040728.
- [32] E. D. Ulker, "A PSO/HS based algorithm for optimization tasks," *2017 Computing Conference SAI*, pp. 117-120, 18-20 July 2017. doi:10.1109/SAI.2017.8252090

- [33] K. -P. Wang, L. Huang, C.-G. Zhou, W. Pang, "Particle swarm optimization for travelling salesman problem," in Proceedings of the 2003 International Conference on Machine Learning and Cybernetics, 5, pp. 1583-1585, November 2003. doi: 10.1109/ICMLC.2003.1259748
- [34] P. Pijarski, P. Kacejko, "Methods of simulated annealing and particle swarm applied to the optimization of reactive power flow in electric power systems," *Advances in Electrical and Computer Engineering*, vol. 18, number 4, pp. 43-48, 2018. doi: 10.4316/AECE.2018.04005
- [35] P. Nammalvar, S. Ramkumar, "Parameter improved particle swarm optimization based direct-current vector control strategy for solar PV system," *Advances in Electrical and Computer Engineering*, vol. 18, number 1, pp. 105-112, 2018. doi: 10.4316/AECE.2018.01013
- [36] H. Fu, Z. Li, Z. Liu, Z. Wang, "Research on big data digging of hot topics about recycled water use on micro-blog based on particle swarm optimization," *Sustainability*, vol. 10, issue 7, 2488, July 2018. doi:10.3390/su10072488
- [37] M. Chih, "Three pseudo-utility ratio-inspired particle swarm optimization with local search for multidimensional knapsack problem," *Swarm and Evolutionary Computation*, vol. 39, pp. 279-296, April 2018. doi:10.1016/j.swevo.2017.10.008
- [38] T. Inan, A. F. Baba, "Particle swarm optimization based collision avoidance," *Turkish Journal of Electrical Engineering and Computer Science*, vol. 27, issue 3, pp. 2137-2155, 2019. doi: 10.3906/elk-1808-63
- [39] J. Robinson, Y. Rahmat-Samii, "Particle swarm optimization in electromagnetics," *IEEE Transactions Antennas and Propagation*, vol. 52, issue 2, pp. 397-407, February 2004. doi: 10.1109/TAP.2004.823969
- [40] S. Ulker, "Particle swarm optimization application to microwave circuits," *Microwave and Optical Technology Letters*, vol. 50, no. 5, pp. 1333-1336, May 2008. doi: 10.1002/mop23369
- [41] S. Ulker, "Broadband microwave amplifier design using particle swarm optimization," *Journal of Computers*, vol. 6, no. 11, pp. 2272-2276, November 2011. doi:10.4304/jcp.6.11.2272-2276
- [42] S. Ulker, "Design of low noise amplifiers using particle swarm optimization," *International Journal of Artificial Intelligence and Applications*, vol. 3, no. 4, pp.99-106, July 2012.
- [43] E. D. Ulker, S. Ulker, "Application of particle swarm optimization to microwave tapered microstrip lines," *Computer Science & Engineering: An International Journal (CSEIJ)*, vol. 4, no. 1, February 2014.
- [44] I. C. Trelea, "The particle swarm optimization algorithm: convergence analysis and parameter selection," *Information Processing Letters*, 85, pp.317-325, 2003. doi: 10.1016/S0020-0190(02)00447-7
- [45] A. Salman, I. Ahmad, S. Al-Madani, "Particle swarm optimization for task assignment problem," *Microprocessors and Microsystems* 26, pp. 363-371, 2002. doi: 10.1016/S0141-9331(02)00053-4
- [46] Q. Lin, J. Li, Z. Du, J. Chen, Z. Ming, "A novel multi-objective particle swarm optimization with multiple search strategies," *European Journal of Operational Research*, vol. 247, issue 3, pp. 732-744, December 2015. doi:10.1016/j.ejor.2015.06.071.
- [47] C. Ma, L. Qu, "Multiobjective optimization of switched reluctance motors based on the design of experiments and particle swarm optimization," *IEEE Transactions on Energy Conversion*, vol. 30, issue 3, pp. 1144-1153, September 2015. doi: 10.1109/TEC.2015.2411677
- [48] J.-L. Duchaud, G. Notton, C. Darras, C. Voyant, "Multi-objective particle swarm optimal sizing of a renewable hybrid power plant with storage," *Renewable Energy*, vol. 131, pp. 1156-1167. February 2019. doi: 10.1016/j.renene.2018.08.058.
- [49] Y. Zhang, Q. Zhang, A. Farnoosh, S. Chen, Y. Li, "GIS-based multi-objective particle swarm optimization of charging stations for electric vehicles," *Energy*, vol. 169, pp. 844-853, February 2019. doi: 10.1016/j.energy.2018.12.062.
- [50] California Institute of Technology, Puff 2.1, Computer Aided Design for Microwave Integrated Circuits. Retrieved 19 November 2017 from: <http://www.its.caltech.edu/~mmic/puffindex/puffE/puffE.htm>
- [51] Rogers Corporation, ROGERS 6006-6010 data sheet. Retrieved: 20 July 2018 from: <http://www.rogerscorp.com/documents/612/index.aspx>
- [52] National Instruments, Vector Network Analyzer PXIe-6532. Retrieved 20 July 2018 from: <https://www.ni.com/en-tr/shop/select/pxi-vector-network-analyzer>